IEEE Access
Multidisciplinary | Rapid Review | Open Access Journal

Received May 14, 2020, accepted May 25, 2020, date of publication June 1, 2020, date of current version June 12, 2020.

Digital Object Identifier 10.1109/ACCESS.2020.2999256

Planar Pyramid Shaped UHF RFID Tag Antenna With Polarisation Diversity for IoT Applications Using Characteristics Mode Analysis

TURKE ALTHOBAITI[1], ABUBAKAR SHARIF[2], JUN OUYANG[2], NAEEM RAMZAN[3], (Senior Member, IEEE), AND QAMMER H. ABBASI[4], (Senior Member, IEEE)

[1]Faculty of Science, Northern Border University, Arar 91431, Saudi Arabia
[2]School of Electronic Science and Engineering, University of Electronic Science and Technology of China, Chengdu 611731, China
[3]School of Computing, Engineering, and Physical Sciences, University of the West of Scotland, Paisley PA1 2BE, U.K.
[4]James Watt School of Engineering, University of Glasgow, Glasgow G12 8QQ, U.K.

Corresponding author: Qammer H. Abbasi (qammer.abbasi@glasgow.ac.uk)

This work was supported in part by the Northern Border University under Grant SCI-2019-1-10-11170, and in part by the University of Glasgow through Engineering and Physical Sciences Research Council (EPSRC) under Grant P/R511705/1.

ABSTRACT This paper presents a novel dual polarised tag antenna design for ultra-high frequency radio frequency identification (UHF RFID) featuring polarisation or frequency band diversity using characteristic mode analysis. The proposed tag design consists of two meandered line bowtie or dipole-like structure (resembles with planar pyramid), shorting stubs, and a ground plane. The initial design comprises of an upper patch wrapped around FR 4 substrate and shorted from all side to ground plane using shorting stubs. After running the characteristic mode analysis of the initial design, the diagonal slots are created to transform the resonant behavior of corresponding characteristic modes towards lower frequency band. However, the characteristics modes of diagonal slots-based structure still shows inductive behavior in US RFID band (902 - 928 MHz). Therefore, the parallel slots having capacitive performance are etched to realise the resonance behaviour of modes in the required RFID band. The positions and dimensions of parallel slots are optimised further to achieve a better conjugate impedance match with RFID chip. Moreover, the frequency band of one or both meandered line dipole-like structures can be tuned to European UHF RFID band by varying the length of the shorting walls. The RFID chip is directly placed at the current minima to run diversity modes. The overall dimensions of the proposed tag antenna are $50 \times 50 \times 2$ mm^3 hence making this dual polarised tag antenna low-cost and easy to fabricate due to the absence of vias, shorting pins, and any matching circuit. Additionally, the proposed tag design offers 3-dB bandwidth ranging from 900 MHz to 940 MHz (40 MHz) together with orientation insensitive 3D read range pattern. The proposed tag design achieved a read range of 5.5 m and 8.5 m on low permittivity dielectric material and 200×200 mm^2 metal plate, respectively.

INDEX TERMS Radiofrequency identification (RFID), UHF tag antenna design, impedance matching, metal mountable tag, polarisation diversity.

I. INTRODUCTION

Radio frequency identification (RFID) and the Internet of Thing (IoT) are transforming this world into a smart planet by converting physical objects into smart devices. RFID with its allied technologies such as IoT, Fifth generation mobile communication network (5G) has been emerging into numerous identification and sensing applications, including retail management, supply chain management, and etc [1]–[5]. Most of these applications require the UHF tags to be mounted on different challenging environment surfaces such as water, wood, metal, and high permittivity dielectric surfaces [6]–[10]. The UHF tags are most promising due to their capability of providing high data transfer rate, long read range, low-cost printable structure [11]–[15]. However, the sensitivity of UHF tags towards different tagging surfaces is quite challenging.

The associate editor coordinating the review of this manuscript and approving it for publication was Renato Ferrero.

In addition to this, some applications such as automatic shopping cart require tag antennas with orientation insensitive features. Most of the commercially available tags consist of linear polarised dipole-like structures, which usually have a quasi-omnidirectional radiation pattern that further leads to orientation sensitivity issues [16]. Therefore, to overcome this sensitivity problem of RFID tags, a circularly polarised reader antenna was usually employed. However, there is a polarisation mismatch loss of 3-dB associated with this linear tag and circular reader antenna. Another possible solution would be designing of tag antenna with circularly polarised characteristics. A circularly polarised UHF RFID tag was proposed in [17] for metallic street pole applications using characteristic mode (CM) analysis. Two CM modes are excited using proximity coupled feed and Wilkinson power divider to achieve 45° main beam direction for ease of reading the tag. However, the size of the street pole tag is large with 90 mm radius and 3 mm substrate thickness, which makes it unsuitable for many low-cost applications.

A circularly polarised (CP) tag antenna based on square-ring and meander strip structure has been proposed in [18]. However, the overall dimensions of this square ring tag are very large $54 \times 54 \times 5.2$ mm^3. In [19], a meandered crossed dipole based CP antenna was proposed for UHF tag or handheld reader applications. This tag design consists of series power divider meandered at the centre and surrounding ring. The surrounding ring acts as a T-match network for impedance matching with RFID chip. The overall design of the tag prototype is $54 \times 54 \times 0.4$ mm^3, with 3-dB axial ratio ranging from 906-932 MHz. A meandered-loop based CP antenna was proposed in [20]. The overall size of 58.6×58.6 mm^2 for CP tag antenna was achieved using meandered loop technique and open gap.

Moreover, this meandered loop design provides a 3-dB axial ratio (AR) bandwidth ranging from 921–929 MHz. So, most of the circular polarised tag antennas usually require execution of two orthogonal modes, which is usually achieved using shorting pins or vias that make this design costly and bulkier. In literature authors proposed dual polarised tag antenna with linear reader antenna to solve orientation sensitivity issues. In [21], a dual polarised dual-planar inverted-F tag antenna with polarisation diversity was proposed. However, this dual PIFA design posed a large footprint $64 \times 64 \times 2$ mm^3. Moreover, the intervention of lumped elements and 12 vias have made this dual PIFA design very complex, since the resonant frequency of this tag design was highly depends on the position of vias. A dipolar patch tag with orientation insensitive capability was proposed in [22]. Although this dipolar patch has compact dimensions, however it has small bandwidth due to very small the real impedance value (3 to 4 Ohms). Also, this tag offers a read range of 3.5 m on metal and less than 2 m on dielectrics. Another metal mountable folded crossed-dipole with polarisation diversity features having dimensions $40 \times 40 \times 1.6$ mm^3 was designed in [23]. This cross dipole based tag has a parasitic metal ring placed beneath the radiator to tune down the resonant frequency that makes this design a bit complex.

Additionally, this tag design shows a read range of 5.6 m to 7.7 m after mounting on different metal objects. Several techniques have been explored in the literature to design dual and circular polarised tag design [11]–[15]. However, CM analysis is becoming the most promising technique due to its forecasting ability of in-depth analysis and systematic procedure towards antenna design. Recently, many types of research employed CM analysis for UHF RFID tag antenna design and many other applications [24]–[32].

Therefore, a dual polarised UHF RFID tag antenna having polarisation or frequency band diversity features has been proposed in this work using CMA to overcome the orientation sensitivity issues. The tag design realised true 3D read range pattern with polarisation diversity and extended read range on metallic objects (even with linearly polarised reader antenna). The proposed tag design comprises of two meandered dipole-like structures, shorting stubs and a ground plane. The diagonal slots are produced in order to shift the resonant behaviour of CM modes towards lower frequency band. Hereafter, almost all modes are still portraying inductive behaviour in the required frequency band. As a result, the small parallel slots (posing capacitive behaviour) are produced to translate the resonance behaviour of modes in the required RFID band. After analysing the characteristics current pattern, the RFID chip was directly placed at the current minima without any other external matching circuit. The antenna dimensions are optimised using CST Microwave studio to attain a conjugate impedance match with Monza 4 D RFID chip from Impinj. Furthermore, the dual polarised tag design offers a read range of 4.5 m and 8.5 m after mounting on low permittivity dielectric materials and 200×200 mm^2 metal plate, respectively.

II. CHARACTERISTIC MODE ANALYSIS (CMA)

Characteristic modes are defined as current modes of conducting objects that depend on their shapes and sizes. CM can be numerically calculated for any arbitrary shaped conducting bodies. Moreover, these current modes are independent of any feed or excitation source and can be obtained by solving eigenvalue equations as follows [33], [34]:

$$X\left(\vec{J_n}\right) = \lambda_n R\left(\vec{J_n}\right) \tag{1}$$

where J_n are eigen currents or eigenfunctions, λ_n are the eigenvalues, X and R are imaginary and real components of MoM impedance matrix, respectively.

As characteristic modes (CM) are orthogonal, so, the total current on antenna surface or any radiating object can be calculated by adding all these characteristic mode currents as follows [17], [25], [26]:

$$J = \sum_n \alpha_n J_n = \sum_n \frac{V_n^i J_n}{1 + \lambda_n} \tag{2}$$

where α_n are the complex modal weighting coefficient (MWC) associated with each mode and can be

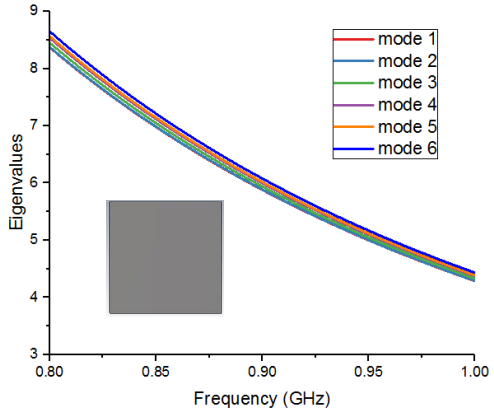

FIGURE 1. Eigenvalue plot of the first six modes of the initial structure.

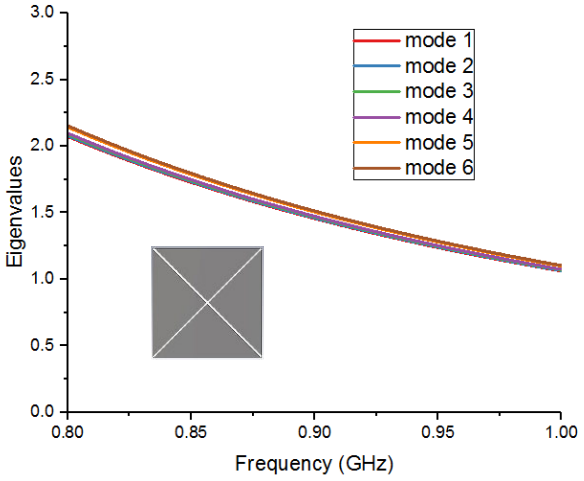

FIGURE 2. Eigenvalue plot of the first six modes of diagonal slots based structure.

calculated as follows [25], [26]:

$$\alpha_n = \frac{V_n^i}{1+\lambda_n} = \frac{\langle E^i, J_n \rangle}{1+\lambda_n} \tag{3}$$

Moreover, the total far-fields associated with total induced currents can also be determined as follows [25]:

$$E = \sum_n \alpha_n E_n$$
$$H = \sum_n \alpha_n H_n \tag{4}$$

where E_n and H_n are radiation far-fields associated with particular characteristic mode current.

Furthermore, the modal significance (MS) can be defined as [25]:

$$MS = \left| \frac{1}{1+\lambda_n} \right| \tag{5}$$

The modal significance is a vital feature of characteristic mode (CM), since it provides information regarding the coupling capability of each CM with external excitation source.

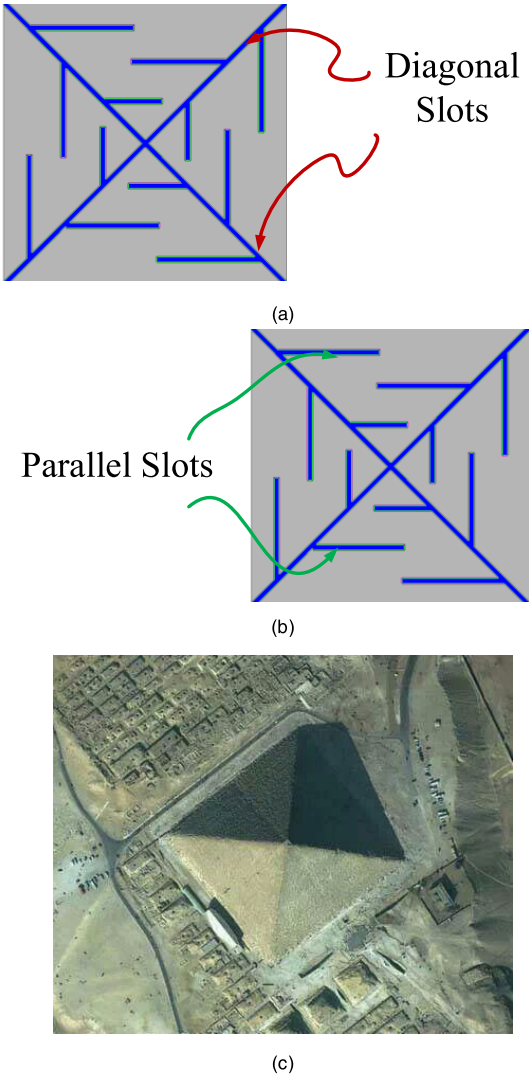

FIGURE 3. Configuration of proposed dual polarised tag antenna design (a) Diagonal slots (b) Parallel slots (c) Resemblance of proposed tag with sky view of Great Pyramid of Giza (https://www.pinterest.com/pin/527695281309724739/).

III. UHF RFID TAG ANTENNA DESIGN USING CMA

The CM analysis of the initial structure was carried out to find the resonant modes and their associated behaviours. The initial structure consists of an upper patch wrapped on 50 × 50 mm^2 FR4-substrate, a ground plane, and shorting walls or stubs connected to ground plane from four sides (as shown in Fig. 1). Fig. 1 shows the eigenvalue plot of the first six modes associated with the initial structure. All six modes depict inductive behaviours in the frequency band of interest ranging from 902 – 928 MHz. More precisely, the modes are initially posing resonating behaviour, somewhere in between 3 to 4 GHz. Therefore, the diagonal slots are created to counter inductive behaviour of modes and further reduce modes resonance towards a relatively lower frequency band, as shown in Fig. 2.

The eigenvalue plot associated with the first six modes of diagonal slot based structure is shown in Fig. 2. The diagonal

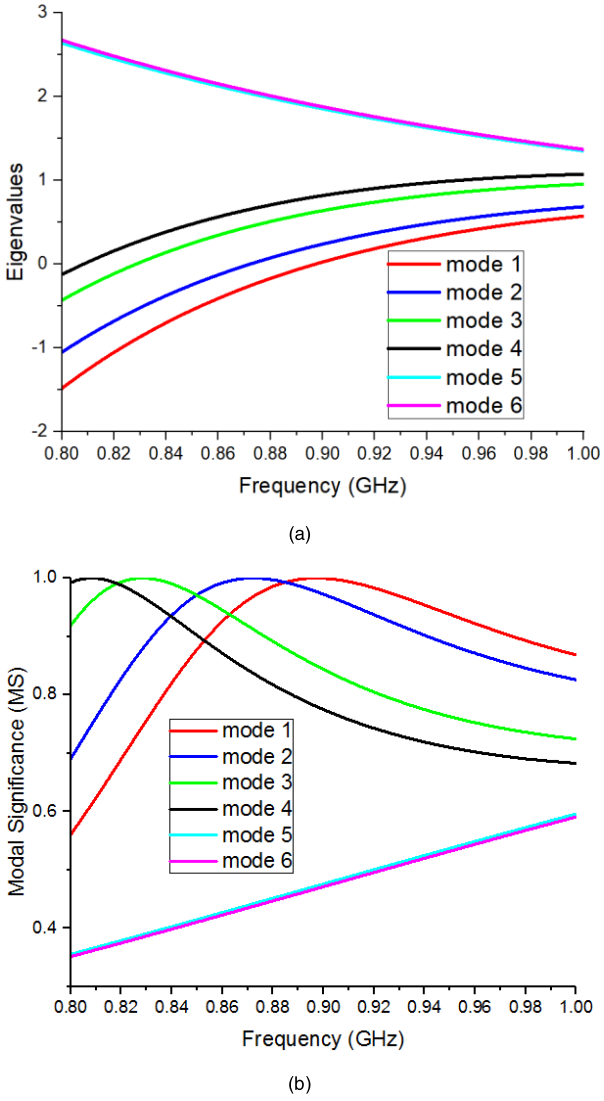

FIGURE 4. (a) Eigenvalue plot of the first six modes of planar pyramid-shaped UHF RFID tag configuration (b) Modal significance plot of the first six modes of planar pyramid-shaped UHF RFID tag configuration.

slot serves two purposes here; one is to scale down the resonant frequencies a bit and counter inductive behaviour. Secondly, it provides the basis for dual UHF RFID tag for either polarisation diversity or frequency band diversity. As can be seen from Fig. 2, the modes still show the inductive behaviour in the frequency band of interest. However, dual polarisation diversity was resulted due to bifurcation of tags into two diagonal bowtie shaped dipoles shorted with ground plane from both ends using short walls/stubs.

To counter the inductive behaviour of modes further, three small parallel slots are added to each wing of bowtie shaped dipole. As a result, the complete tag configuration resembles with sky view of the Great Pyramid of Giza, as shown in Fig. 3.

The eigenvalue plot of the first six modes of planar pyramid-shaped tag configuration with two diagonal and three parallel slots at each wing are shown in Fig. 4(a).

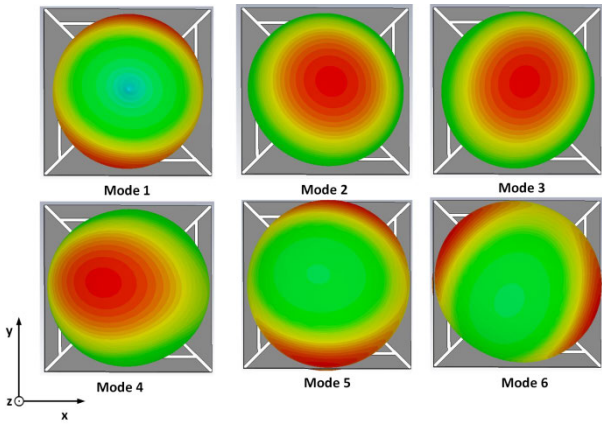

FIGURE 5. Characteristics far-field pattern of the first six modes of pyramid-shaped tag antenna.

The modes 1, 2, 3 and 4 show resonant behaviours near frequency band of interest. However, the modes 5, and 6 again show inductive behaviour. To validate it further, the modal significance plot of the first six modes was also depicted in Fig. 4(b). First four modes are significant modes since their ($MS > 1/\sqrt{2}$). While modes 5 and 6 are non-significant modes due to their ($MS < 1/\sqrt{2}$). As a result, mode 1, 2, 3 and 4 show resonant behaviour in required frequency band along with MS value approaches to 1 (significant modes). Therefore, polarisation or frequency band diversity can be achieved by carefully exciting two or more modes (among 1, 2, 3 and 4).

To explore it further, the characteristics far-field pattern of each mode is shown in Fig. 5. The characteristics far-field pattern helped us in deciding the modes that must be excited carefully in order to achieve polarisation diversity. For mode 1, it shows radiation along the shorted walls of tag design along with a null in + Z direction. Mode 2 and 3 have an orthogonal far-field pattern, which is pivotal for polarisation diversity. Similarly, mode 3 and 4 can also be excited to produce polarisation diversity; however, this pair needs further optimisation of parameters. Moreover, mode 5 and 6 are not depicting any useful feature regarding polarisation diversity or read range enhancement. It is worth to mention here that mode 1 observed a field cancellation in + z-direction. However, it provides good far-field characteristics along shortened sides of UHF tags. This fact can be exploited to get a true 3 D radiation pattern and hence enables the reading of tag from different orientations, even from upper and lower sides of the tag. Furthermore, to excite particular modes and to find a suitable location for RFID chip placement for polarisation diversity, the characteristics currents related to corresponding modes of pyramids tag structure are shown in Fig. 6. The mode 1 represents symmetric current distribution that resulted into cancellation of the field in the + z-direction. Mode 2 poses strong current distribution only along horizontal dipole, which is pivotal for far-field in the horizontal direction. Similarly, mode 3 shows strong current distribution along vertical dipoles and weak current distribution in

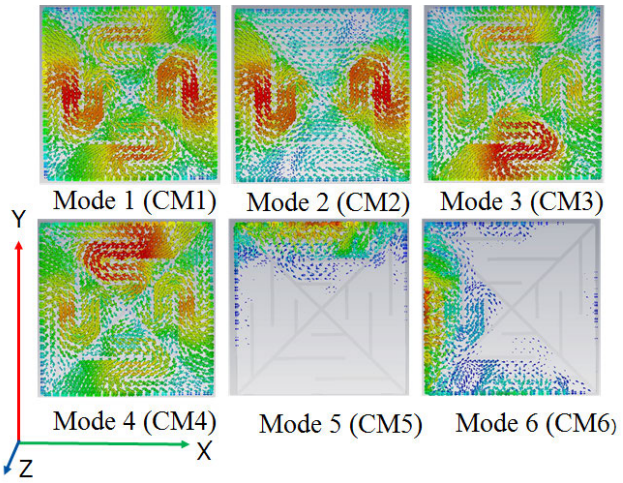

FIGURE 6. Characteristics current distribution related to the first six modes of pyramid-shaped tag antenna.

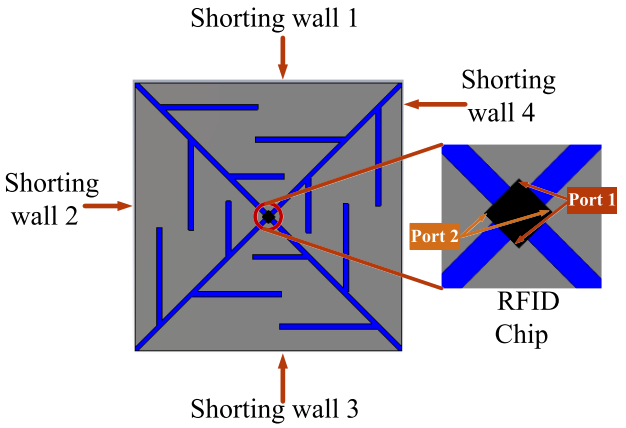

FIGURE 7. Dual polarised tag configuration with shorting stubs resulted after CMA.

horizontal dipoles. The mode 4 also shows strong current distribution long vertical dipoles along with week current distribution in the horizontal dipole. In addition, mode 4 has a weak vertical current distribution as compared to mode 3. Modes 5 and 6 do not have good current distribution, which leads to weak far-field characteristics. According to [28] and [35], to excite a particular mode, inductive coupling element (ICE) must be placed at current maxima. Conversely, to excite a mode, capacitive coupling element (CCE) must be placed at current minima. In our case, since RFID chip is inherently a capacitive element. So, we placed RFID chip at current minima directly to excite particular modes. The placement of RFID chip directly at current minima provides an additional benefit that is to avoid any matching circuit or balun for chip impedance matching, which is vital for cost saving in RFID tags. As can be seen from Fig. 6, the mode 2 and 3 are the most promising modes for polarisation diversity. So, this mode pair (2, 3) must be excited to achieve polarisation diversity. The modes 2 and 3 current distribution shows current minima at the tip of the pyramid-shaped wing. Therefore, the RFID chip must be placed at this point to excite modes 2 and 3. It is worth to mention here, after placing the RFID chip at the tip, it will also excite other modes partially such as mode 1 and 4 since these modes also have current minima near the tip of the pyramid-shaped wing. Finally, the proposed antenna configuration resulted after CMA is shown in Fig. 7.

To understand which modes will be stimulated by port excitation and to compare characteristic modes performance, the CM analysis was performed by placing a CCE as port 1 along with horizontal pyramid wings. Consequently, the normalised MWC amplitude by exciting only port 1 attached to a horizontal pyramid dipole wing is shown in Fig. 8 (a). The port 1 CCE excites mode 2 more efficiently along with excitation of modes 3 and 4 partially. However, the normalised MWC shows mode 2 is more significant mode as compared to mode 3 and 4.

Similarly, the normalised MWC resulted after placing CCE at port 2 is shown in Fig. 8 (b). Accordingly, the port 2 CCE excites mode 3 more efficiently along with excitation of modes 4 partially. An interesting phenomenon occurs after exciting both port 1 and 2 using CCE. The normalised MWC amplitude for both port excitations simultaneously is shown in Fig. 8 (c). This dual-port configuration excites mode 2 and 3 efficiently and modes 1 and 4 partially. To understand why the mode 1 partially excited with dual-port configuration, let us refer to Fig. 6 of characteristics current distribution associated with mode 1. The mode also shows approximate current minima at tips of pyramid dipole wings. The mode 1 excited partially since the actual current minima of mode 1 occurs at four corners due to current cancellation. The partial excitation of mode 1 is very advantageous due to providing the capability of reading the tag from different sides.

IV. SIMULATION AND MEASUREMENT RESULTS

The dimensions of the dual polarised UHF RFID tag are optimised further using the full-wave simulation option of CST Microwave studio. Fig. 9 illustrates the dimensions and geometry of the proposed dual polarised UHF RFID tag antenna. The value of each dimension is expressed in the caption of Fig. 9. Moreover, the effect of substrate thickness on tag performance has also been studied as shown in Fig. 10. The thickness of the substrate varied from 1 mm to 4 mm. It can be observed that changing the thickness of the substrate changes the width of the shorting wall/stub, which is an essential parameter in determining the impedance of the tag. Consequently, the increase in the thickness of the substrate (t) produces a mismatch matching between RFID chip and tag impedance due to an increase in the imaginary part of the tag, as shown in Fig. 10. The real impedance of the tag decreases as the thickness of the substrate increases.

However, the radiation efficiency of the tag improves with an increase in the thickness of the substrate. Since the increase in substrate thickness increases the distance between the

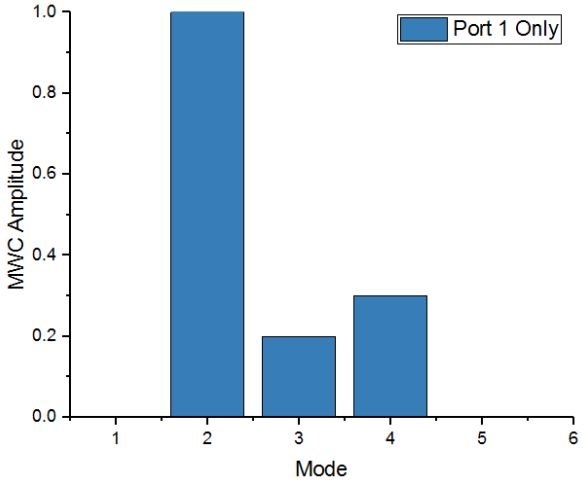

(a)

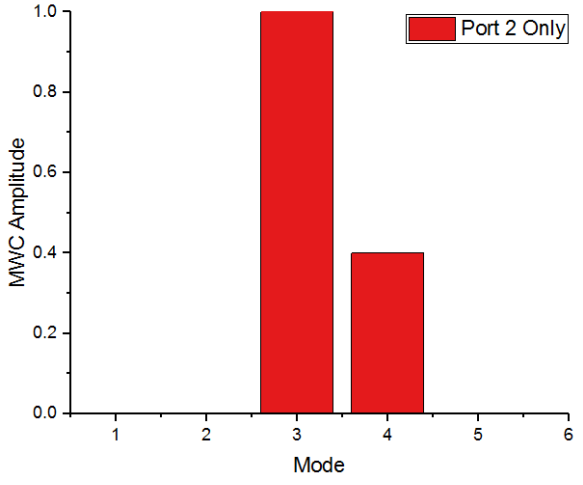

(b)

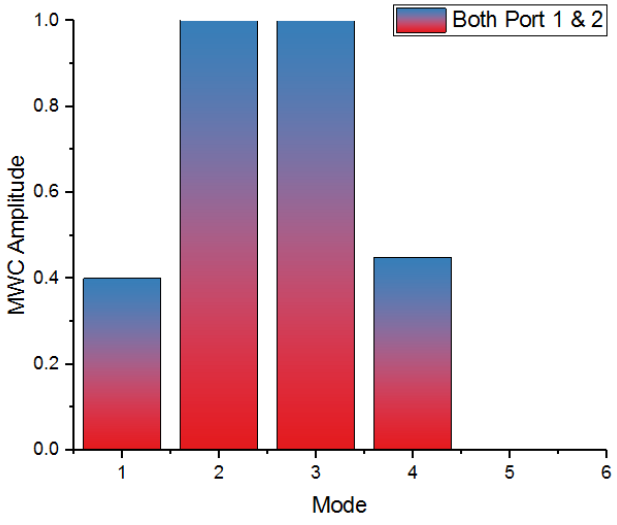

(c)

FIGURE 8. Normalised MWC amplitude by exciting (a) Only Port 1 attached to horizontal pyramid dipole wing (b) Only Port 2 attached to vertical pyramid dipole wing (c) Both ports attached simultaneously.

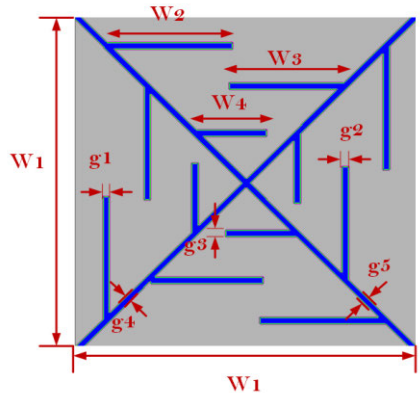

FIGURE 9. Geometry and dimensions of proposed dual-polarized UHF RFID tag antenna (W1 = 50, W2 = 18.36, W3 = 16.86, W4 = 10.36, g1 = 1, g2 = 1, g3 = g4 = g5 = 1).

tag and metallic plane. As a result, the radiation efficiency improves. On the other hand, the imaginary impedance and radiation efficiency of the tag are decreasing as the thickness of the substrate decreases. So, the optimal value of substrate thickness was taken as 2 mm. The simulated imaginary and real impedance of dual polarised tag antenna for both ports are shown in Fig. 11 (a). The imaginary impedance is ranging from 140 Ω to 150 Ω in the required frequency band, while real impedance is ranging from 5 Ω to 8 Ω in the US RFID band. According to the datasheet, the real impedance of Impinj Mona 4 D chip is 11-143 j at 915 MHz [36]. The imaginary part of the tag antenna is matched well to counter the imaginary part of the Monza 4 D RFID tag chip. However, the real impedance of the tag antenna is a bit less as compared to the real impedance of the chip. Similarly, the S11 or S22 parameter for both ports after mounting on 200 × 200 mm2 metal plate is depicted in Fig. 11 (b). The tag antenna achieved 3-dB bandwidth ranging from 900 MHz to 940 MHz (approx., 40 MHz). Also, the S21 or S12 parameter or isolation between two ports is shown in Fig. 11(b).

The value of S21 parameter around −45 dB in the frequency band of interest shows excellent isolation between two ports of the proposed tag antenna. Additionally, the performance of proposed tag antenna such as impedance, S11 and S22 parameter remains same either in free space or after mounting on 200 × 200 mm^2 metal plate. The performance of proposed tag remains intact even on low permittivity dielectric materials (relative permittivity values ranging from 1 to 7). To prove the concept of dual polarisation, the surface current distribution and far-field radiation pattern of dual polarised configuration are obtained by running the full-wave simulation (frequency-domain solver of CST MWS), as shown in Figs 12 (a) and (b), respectively. Fig. 12 reveals that the surface current distribution and associated far-field of the proposed antenna due to two ports are orthogonal to each other. Thereby, it validates the concept of proposed tag design using CMA, and further proves the significance of the tag.

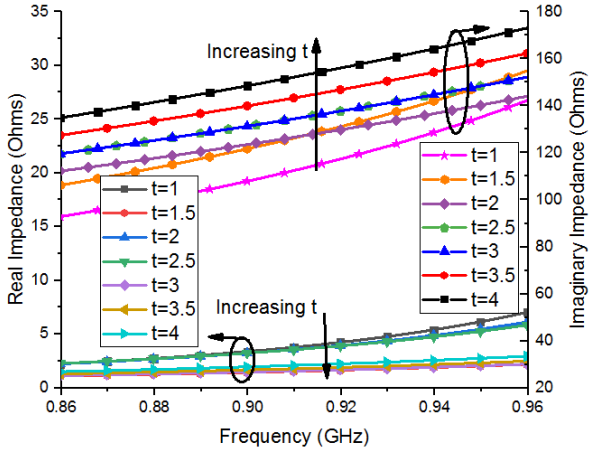

FIGURE 10. Simulated real and imaginary impedance of the proposed dual polarised tag antenna with different substrate thickness (t) values.

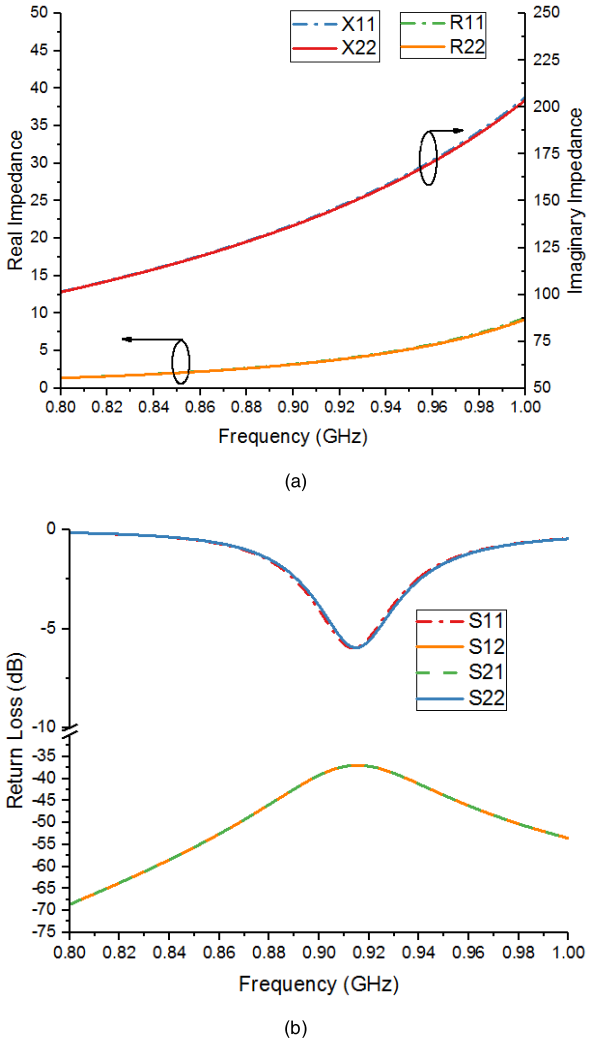

FIGURE 11. (a) Simulated real and imaginary impedance plot of two ports of proposed dual polarised UHF RFID tag antenna after mounting on 200 x 200 mm^2 metal plate (b) S11 plot and isolation S21 between two ports of proposed dual polarised UHF RFID tag antenna after mounting on 200 x 200 mm^2 metal plate.

Towards orientation insensitive IoT applications. Another frequency band diversity option can be achieved by adjusting the length of shorting stub of the pyramid dipole wing (as shown in Figure 13). If the length of both shorting stubs of the pyramid dipole wings is shortened to 29.4 mm, the frequency band of one dipole structure was shifted to European RFID frequency band (860 to 865 MHz). Hence, the proposed tag can be able to provide two diversity options either for polarisation or frequency band diversity. To validate it further, a prototype of the proposed dual polarised RFID tag antenna was fabricated (printed on FR4 substrate), as shown in Figure 14. The FR4 substrate having a thickness of 2 mm, a dielectric constant ($\varepsilon_r = 4.4$), and a loss tangent of ($\tan\delta = 0.02$) was used to fabricate the antenna. The Impinj Monza 4 D chip is connected among all four terminals of tag antenna, as mentioned in the datasheet.

To corroborate the performance of the antenna, the input impedance of this dual polarised tag has been measured by following the procedure expressed in [37] and [25] using Agilent E8363B vector network analyser. Two coaxial cables were employed for impedance and return loss measurement, with outer coats of coaxial cables are soldered together. In contrast, the inner conductor of each cable has been connected with open ends of the tag antenna without chip mounting. The measured return loss of the proposed dual polarised tag antenna has been calculated by using the formula in [37]. Fig. 15 shows the comparison of measured and simulated S11 and port isolation parameters of the proposed tag. It can be observed that the measured S11 or S22 shows a good agreement with the simulated one. However, there is a little bit shift in measured S11.

On the other hand, the measured S11 is much better than the simulated one, which may be due to an increase in loss factor or permittivity value of FR4 substrate from values used for simulation purposes. Moreover, the measured isolation S21 between two ports is also decreased up to -15 dB, which is acceptable. The decrease in isolation S21 may be resulted due to cable loss or some other fabrication error.

Fig. 16 shows the simulated and measured realized gains of the proposed tag antenna ($\theta = 0°$, $\phi = 90°$). It can be observed that the tag antenna can offer a maximum simulated realized gain of -4.87 dBi at 917 MHz. However, the tag antenna achieved a maximum measured realized gain of -6.05 dBi at 910 MHz. The measured and simulated realized gains are matched well with a difference in resonant frequency, and gains are only 7 MHz and 1.18 dB, respectively.

V. READ RANGE TESTING

Fig. 17 shows the read range measuring Tagformance pro setup from Voyantic Company that was deployed for read range measurement of the proposed tag. This setup consists of a foam spacer, a linear polarised antenna with 6 dBi gain,

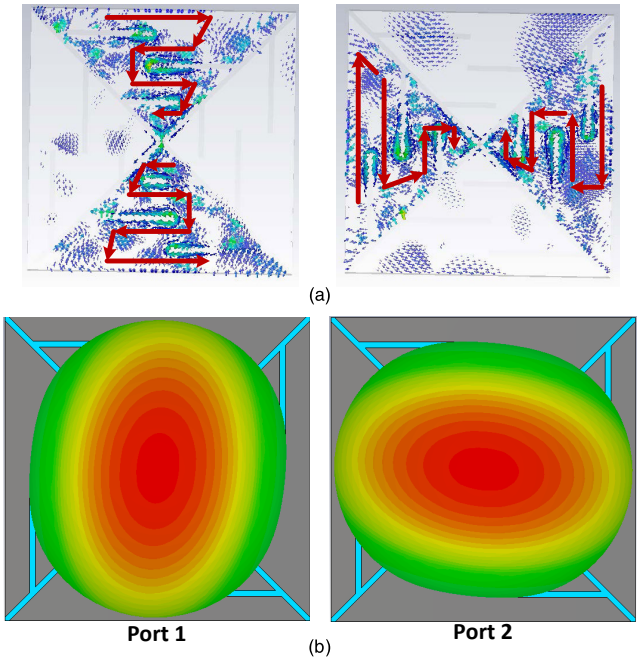

FIGURE 12. (a) Surface current distribution of two ports of proposed dual polarised UHF RFID tag antenna (b) Far-field pattern of two ports of proposed dual polarised UHF RFID tag antenna.

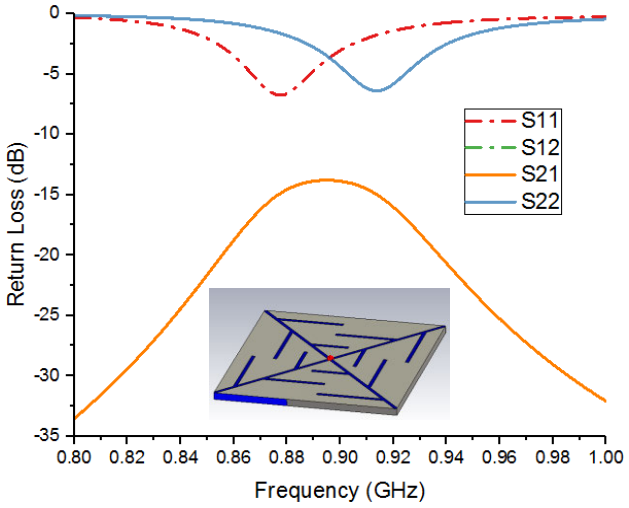

FIGURE 13. S11 plot and isolation S21 between two ports of proposed dual polarised tag antenna with frequency band diversity option after mounting on 200 x 200 mm^2 metal plate.

and laptop with software setup to estimate the measured read range. The setup works by running a frequency sweep, and a foam spacer stipulates the fixed distance between the reader antenna and tag (d_{ref}).

The theoretical read range can be estimated using the following formula:

$$d_{\max} = d_{ref}\sqrt{\frac{EIRP_{\max}}{EIRP_{ref}}} \tag{6}$$

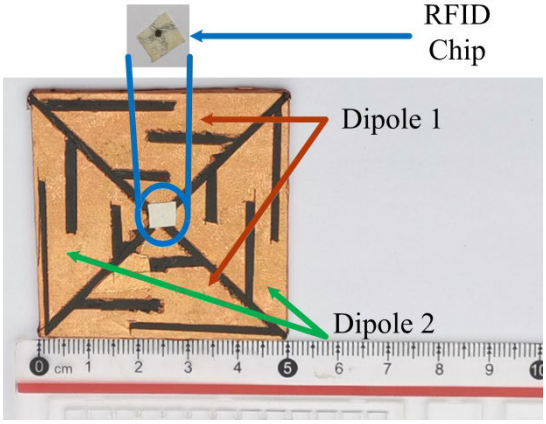

FIGURE 14. A fabricated prototype of proposed dual polarised UHF RFID tag antenna.

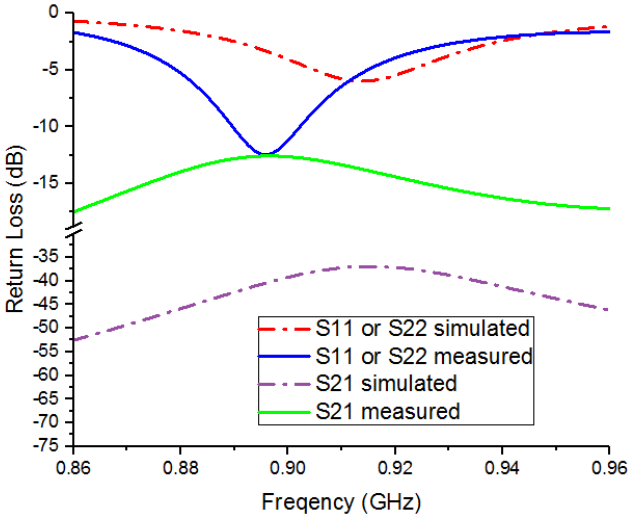

FIGURE 15. Measured and simulated S11 plot and isolation S21 between two ports of proposed dual polarised UHF RFID tag antenna.

where d_{ref} and $d_{\max}$ are the fixed distance specified by foam spacer and maximum reading distance of the tag, respectively. $EIRP_{\max}$ is the maximum permitted EIRP = 4 Watts for most of the regions, and $EIRP_{ref}$ is the reference EIRP of the range measuring setup.

Fig. 18 shows the fabricated tag antenna mounted on 200 × 200 mm^2 metal plate. The measured read range of this dual polarised tag antenna in free space and after mounting above 200 × 200 mm^2 metal sheet is depicted in Fig. 19. The measured read range pattern vs different angles in XY-plane demonstrates the ability of the proposed tag to achieve true 3 D read pattern. The proposed tag antenna achieved a read range of 8.5 m and 5.5 m on a metal plate and free space, respectively. Additionally, due to excitation of mode 1, this tag antenna can be readable up to 1.5 m from upper, lower, right and left sides of the tag.

To verify the robustness of the proposed tag antenna, the read range is measured after mounting the tag on

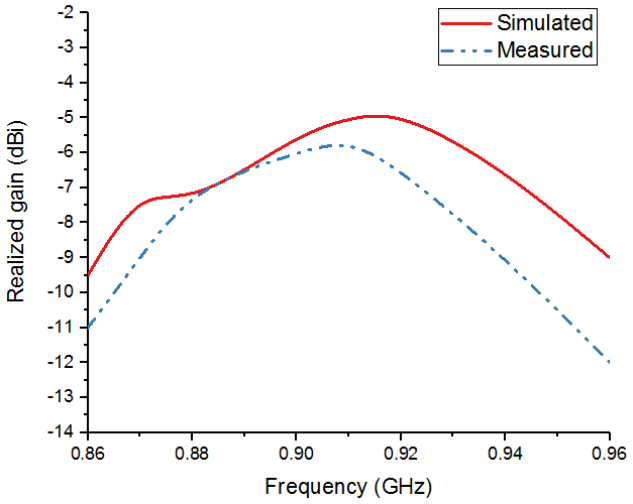

FIGURE 16. Simulated and measured realized gains of proposed tag antenna after mounting on 200 × 200 mm^2 metal plate.

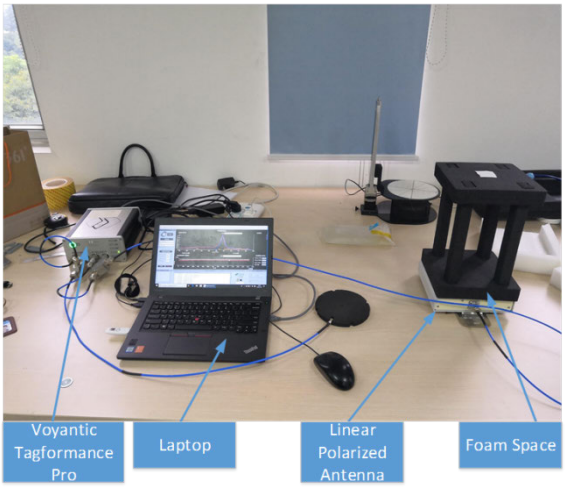

FIGURE 17. Read range measuring Tagformance pro setup from Voyantic Company.

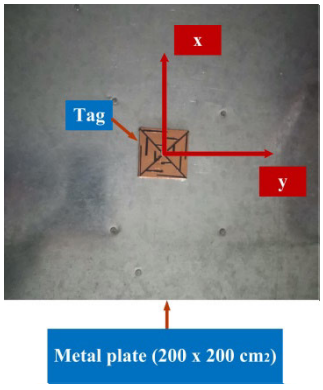

FIGURE 18. Measured and simulated S11 plot and isolation S21 between two ports of proposed dual polarised UHF RFID tag antenna.

metallic objects of different sizes and shapes, as depicted in Fig. 20. The read range of proposed dual polarised tag antenna has been measured by placing these items in different

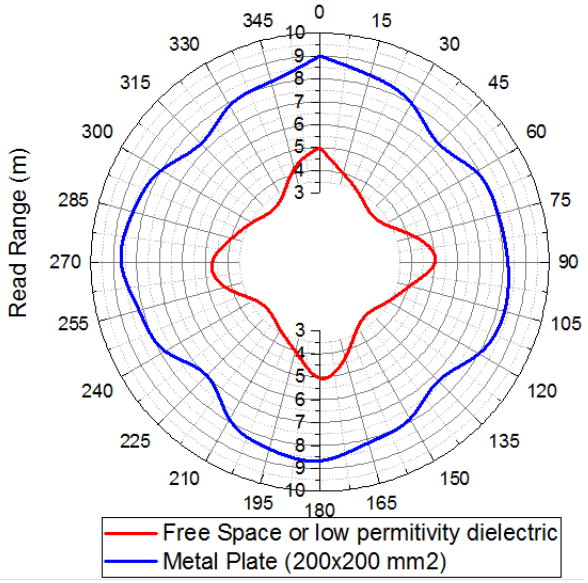

FIGURE 19. Measured read range of proposed antenna in XY plane at 910 MHz.

FIGURE 20. Metallic Objects of different shapes and sizes.

orientations, as shown in Fig. 21, and successfully read by a linearly polarised reader antenna. The read range is measured by setting the maximum EIRP to 4 W.

It can be seen that the read range of tag on olive oil metallic container is maximum 7 m, while the read range of the tag on small candy container is 4.5 m. Correspondingly; the read range of proposed tag antenna on milk powder container and metallic hot water bottle is 6 m and 5.2 m, respectively.

Table 1 shows the comparison of proposed tag antenna with state of the art published work including dual-polarized, CP and platform tolerant tag antennas. Although the dual polarised dual-planar inverted-F tag antenna with polarisation diversity was proposed in [21] can achieve more read range up to 10.2 m. However, this dual PIFA design has a large footprint 64 × 64 × 2 mm^3 as compared to our design.

TABLE 1. Comparison of the proposed tag antenna with other state of the art.

Ref.	Tag Dimensions (mm3)	Substrate	Backing Plate Size (mm2)	Max. Read Range by LP Reader Antenna (m)	3-dB bandwidth	Dual Polarized	Platform Tolerant	Cover US + European RFID Band	Vias Or Shorting pin
This work	50 × 50 × 2	FR4 (ε_r = 4.4)	200 × 200	8.5	40 MHz	Yes	Yes	Yes (Tunable)	No
[21]	64 × 64 × 2	FR4 (ε_r = 4.4)	200 × 200	10.2	Small	Yes	Yes	No	Yes (12 Vias)
[22]	30 × 30 × 1.6	PET + Softlon (ε_r = 1.06)	200 × 200	3.5	Small (real impedance < 5 Ω)	Yes	Yes	No	No
[23]	40 × 40 × 1.6	polyimide film (ε_r = 3.3) + Foam (ε_r = 1.06)	200 × 200	7.7	Small	Yes	Yes	No	No, (parasitic metal ring)
[19]	56 × 56 × 0.4	FR4 (ε_r = 4.6)	--	7 (free space)	--	CP	No	Yes	No
[20]	58.6 × 58.6 × 0.4	FR4 (ε_r = 4.4)	--	15.5	--	CP	No	No	No
[38]	35.6 × 35.6 × 0.508	Rogers RO4003 (ε_r = 3.2)	--	5.7	--	CP	No	No	No
[39]	58 × 58 × 1.6	FR4 (ε_r = 4.4)	--	10.9	--	CP	No	No	No
[40]	180 × 36 × 2.5	GML 1100 woven-glass + foam	--	15.8 (free space)	--	No	Yes	No	No
[41]	80 × 60 × 0.76	GIL GM 1000 (ε_r = 3.2)	150 × 150	5.4	--	No	Yes	No	No

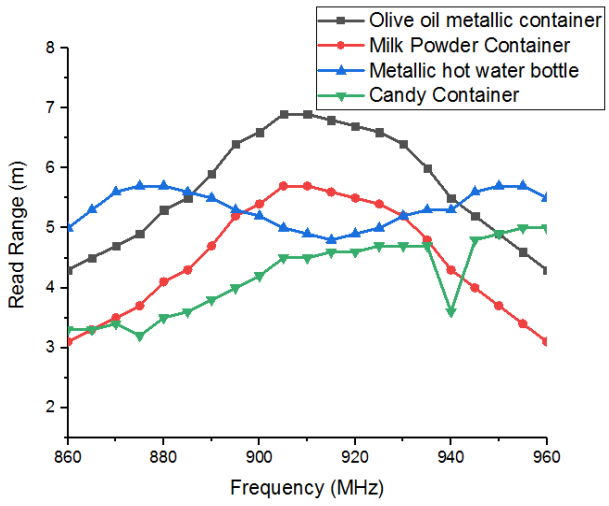

FIGURE 21. Measured read range of proposed tag on different metallic objects.

Moreover, the involvement of lumped elements and 12 vias have made this dual PIFA design very complex and costly. Also, the resonant frequency of this tag design highly depended on the position of vias.

The size of the dipolar patch tag presented in [22] is small (along with orientation insensitive capability). However, it has small bandwidth due to very small the real impedance value (3 to 4 Ohms) and therefore poses a poor impedance matching with RFID chip. Also, this tag offers a read range of 3.5 m on metal and less than 2 m on dielectrics. The metal mountable folded crossed-dipole in [23] has dimensions 40 × 40 × 1.6 mm^3 (along with polarisation diversity features). This cross dipole based tag has a parasitic metal ring placed beneath the radiator to tune down the resonant frequency that makes this design a bit complex. Additionally, this tag design shows a read range of 5.6 m to 7.7 m after mounting on different metal objects.

In addition to this, we also compared our design with some of the cross dipole based circular polarized (CP) antennas published in [19], [20] and [38], [39], which usually consist of a single-layer substrate without a ground plane, therefore not suitable for platform tolerant or metal mountable applications. Some other cross-dipole based antennas presented in [21]–[23] are suitable for platform tolerant or metal mountable applications. However, most of these antennas have very low-real impedance and have small 3 dB bandwidth.

The proposed dual-polarized tag antenna achieved a 3 dB bandwidth of more than 40 MHz along with a frequency band tunable feature. It can be tuned to the European RFID band by varying the length of the shorting wall. Also, our proposed tag does not require the use of vias/shorting pins, lumped elements, and parasitic metal ring to shrink down the frequency. Furthermore, the proposed tag design achieved a read range of 5.5 m and 8.5 m on low permittivity dielectric material and 200 × 200 mm^2 metal plate, respectively. So, the proposed tag antenna planar pyramid-shaped (can also

be considered as a cross dipole) show a clear advantage compared to other state of the art.

VI. CONCLUSION

In this paper, a dual polarised UHF RFID tag antenna having polarisation or frequency band diversity features have been proposed using CMA. The proposed tag antenna consists of two meandered line cross dipole-like structures, shorting stubs, and a ground plane. The overall configuration of the proposed tag is inspired by planar pyramid structure. By exploring characteristic modes analysis, the diagonal slots and parallel slots (posing capacitive behaviour) are created to transform the resonant behaviour of CM modes in the required RFID band. The length and positions of parallel slots are optimised further to obtain the conjugate impedance match with Monza 4D chip. Moreover, the frequency band diversity is achieved by employing the shorting wall's length as a tuning parameter. The frequency band of one or both meandered line dipole-like structure can be tuned to European UHF RFID band by varying the length of the shorting wall. The RFID chip is directly placed at the current minima to run diversity modes. This tag design is low cost and easy to fabricate due to absence of vias, shorting pins and any matching circuit. The size of the proposed tag antenna is $50 \times 50 \times 2$ mm^3. Furthermore, the proposed tag design achieved a read range of 8.5 m after mounted above 200×200 mm^2 metal plate. Similarly, it achieved a read range of 5.5 m on low permittivity dielectric material. The robustness of the proposed tag solution is also verified after mounting it on metallic objects of different shapes and sizes. Consequently, the proposed tag antenna is suitable for platform tolerant and orientation insensitive IoT applications.

REFERENCES

[1] E. Perret, S. Tedjini, and R. S. Nair, "Design of antennas for UHF RFID tags," *Proc. IEEE*, vol. 100, no. 7, pp. 2330–2340, 2012.

[2] A. Sharif, J. Ouyang, F. Yang, H. T. Chattha, M. A. Imran, A. Alomainy, and Q. H. Abbasi, "Low-cost inkjet-printed UHF RFID tag-based system for Internet of Things applications using characteristic modes," *IEEE Internet Things J.*, vol. 6, no. 2, pp. 3962–3975, Apr. 2019.

[3] H. Li, J. Zhu, and Y. Yu, "Compact single-layer RFID tag antenna tolerant to background materials," *IEEE Access*, vol. 5, pp. 21070–21079, 2017.

[4] A. Sharif, J. Guo, J. Ouyang, S. Sun, K. Arshad, M. A. Imran, and Q. H. Abbasi, "Compact base station antenna based on image theory for UWB/5G RTLS embraced smart parking of driverless cars," *IEEE Access*, vol. 7, pp. 180898–180909, 2019.

[5] H. Farhat, P. Iliev, P. Marriage, and N. Rolland, "An added value alternative to RAIN RFID items characterization in retail," *IEEE Access*, vol. 6, pp. 32430–32439, 2018.

[6] S.-L. Chen, "A miniature RFID tag antenna design for metallic objects application," *IEEE Antennas Wireless Propag. Lett.*, vol. 8, pp. 1043–1045, 2009.

[7] S.-L. Chen and K.-H. Lin, "A slim RFID tag antenna design for metallic object applications," *IEEE Antennas Wireless Propag. Lett.*, vol. 7, pp. 729–732, 2008.

[8] H.-D. Chen and Y.-H. Tsao, "Low-profile PIFA array antennas for UHF band RFID tags mountable on metallic objects," *IEEE Trans. Antennas Propag.*, vol. 58, no. 4, pp. 1087–1092, Apr. 2010.

[9] B. Lee and B. Yu, "Compact structure of UHF band RFID tag antenna mountable on metallic objects," *Microw. Opt. Technol. Lett.*, vol. 50, no. 1, pp. 232–234, Jan. 2008.

[10] H.-W. Son and S.-H. Jeong, "Wideband RFID tag antenna for metallic surfaces using proximity-coupled feed," *IEEE Antennas Wireless Propag. Lett.*, vol. 10, pp. 377–380, 2011.

[11] D. M. Dobkin, *The RF in RFID?: UHF RFID in Practice*. Amsterdam, The Netherlands: Elsevier, 2013.

[12] Q. Liu, H. Li, and Y.-F. Yu, "A versatile flexible UHF RFID tag for glass bottle labelling in self-service stores," *IEEE Access*, vol. 6, pp. 59065–59073, 2018.

[13] M. Fischer, M. Ferdik, L.-O. Rack, G. Saxl, M. Renzler, and T. Ussmueller, "An experimental study on the feasibility of a frequency diverse UHF RFID system," *IEEE Access*, vol. 7, pp. 132311–132323, 2019.

[14] M. Švanda and M. Polívka, "Two novel extremely low-profile slot-coupled two-element patch antennas for UHF RFID of people," *Microw. Opt. Technol. Lett.*, vol. 52, no. 2, pp. 249–252, Feb. 2010.

[15] M. Svanda and M. Polivka, "Matching technique for an on-body low-profile coupled-patches UHF RFID tag and for sensor antennas," *IEEE Trans. Antennas Propag.*, vol. 63, no. 5, pp. 2295–2301, May 2015.

[16] Q. Zhang, M. J. Crisp, R. V. Penty, and I. H. White, "Reduction of proximity effects on UHF passive RFID systems by using tags with polarization diversity," *IEEE Trans. Antennas Propag.*, vol. 63, no. 5, pp. 2264–2271, May 2015.

[17] Y. Yan, J. Ouyang, X. Ma, R. Wang, and A. Sharif, "Circularly polarized RFID tag antenna design for metallic poles using characteristic mode analysis," *IEEE Antennas Wireless Propag. Lett.*, vol. 18, no. 7, pp. 1327–1331, Jul. 2019.

[18] J.-H. Lu and B.-S. Chang, "Planar compact square-ring tag antenna with circular polarization for UHF RFID applications," *IEEE Trans. Antennas Propag.*, vol. 65, no. 2, pp. 432–441, Feb. 2017.

[19] D. Inserra and G. Wen, "Compact crossed dipole antenna with meandered series power divider for UHF RFID tag and handheld reader devices," *IEEE Trans. Antennas Propag.*, vol. 67, no. 6, pp. 4195–4199, Jun. 2019.

[20] H.-D. Chen, C.-Y.-D. Sim, C.-H. Tsai, and C. Kuo, "Compact circularly polarized meandered-loop antenna for UHF-band RFID tag," *IEEE Antennas Wireless Propag. Lett.*, vol. 15, pp. 1602–1605, 2016.

[21] E. Yang and H. Son, "Dual-polarised metal-mountable UHF RFID tag antenna for polarisation diversity," *Electron. Lett.*, vol. 52, no. 7, pp. 4–5, 2016.

[22] F.-L. Bong, E.-H. Lim, and F.-L. Lo, "Compact orientation insensitive dipolar patch for metal-mountable UHF RFID tag design," *IEEE Trans. Antennas Propag.*, vol. 66, no. 4, pp. 1788–1795, Apr. 2018.

[23] P. Diversity and U. H. F. Tag, "Compact folded crossed—dipole for on—metal," *IEEE J. Radio Freq. Identif.*, vol. 4, no. 2, pp. 115–123, Jun. 2020.

[24] A. Sharif, J. Ouyang, M. A. Imran, and Q. H. Abbasi, "Orientation insensitive UHF RFID tag antenna with polarization diversity using characteristic mode analysis," in *Proc. IEEE Int. Symp. Antennas Propag. USNC-URSI Radio Sci. Meeting*, Atlanta, GA, USA, Jul. 2019, pp. 7–12.

[25] A. Sharif, J. Ouyang, F. Yang, R. Long, and M. K. Ishfaq, "Tunable platform tolerant antenna design for RFID and IoT applications using characteristic mode analysis," *Wireless Commun. Mobile Comput.*, vol. 2018, pp. 1–10, May 2018.

[26] Y. Gao, R. Ma, Q. Zhang, and C. Parini, "Design of very-low-profile circular UHF small antenna using characteristic mode analysis," *IET Microw., Antennas Propag.*, vol. 11, no. 8, pp. 1113–1120, Jun. 2017.

[27] R. Martens and D. Manteuffel, "Systematic design method of a mobile multiple antenna system using the theory of characteristic modes," *IET Microw., Antennas Propag.*, vol. 8, no. 12, pp. 887–893, Sep. 2014.

[28] R. Martens, E. Safin, and D. Manteuffel, "Selective excitation of characteristic modes on small terminals," in *Proc. 5th Eur. Conf. Antennas Propag. (EUCAP)*, Apr. 2011, pp. 2492–2496.

[29] Z. Liang, J. Ouyang, M. Gao, and X. Cui, "A small RFID tag antenna for metallic object using characteristic mode," in *Proc. IEEE Int. Symp. Antennas Propag. USNC/URSI Nat. Radio Sci. Meeting*, Jul. 2017, pp. 533–534.

[30] Z. Liang, J. Ouyang, F. Yang, and L. Zhou, "Design of license plate RFID tag antenna using characteristic mode pattern synthesis," *IEEE Trans. Antennas Propag.*, vol. 65, no. 10, pp. 4964–4970, Oct. 2017.

[31] A. Sharif, M. Ali Imran, J. Ouyang, Q. H. Abbasi, and Y. Yan, "Circular polarized RFID tag antenna design using characteristic mode analysis," in *Proc. Int. Workshop Antenna Technol. (iWAT)*, Mar. 2019, pp. 62–64.

[32] F. A. Dicandia, S. Genovesi, and A. Monorchio, "Efficient excitation of characteristic modes for radiation pattern control by using a novel balanced inductive coupling element," *IEEE Trans. Antennas Propag.*, vol. 66, no. 3, pp. 1102–1113, Mar. 2018.

[33] M. Cabedo-Fabres, E. Antonino-Daviu, A. Valero-Nogueira, and M. Bataller, "The theory of characteristic modes revisited: A contribution to the design of antennas for modern applications," *IEEE Antennas Propag. Mag.*, vol. 49, no. 5, pp. 52–68, Oct. 2007.
[34] Y. Chen and C. F. Wang, *Characteristic Modes: Theory and Applications in Antenna Engineering*. Hoboken, NJ, USA: Wiley, 2015.
[35] R. Martens, E. Safin, and D. Manteuffel, "Inductive and capacitive excitation of the characteristic modes of small terminals," in *Proc. Loughborough Antennas Propag. Conf.*, Nov. 2011, pp. 4–7.
[36] *Monza 4, Tag Chip Datasheet, Version 10.0*, Impinj, Seattle, WA, USA, 2016.
[37] X. Qing, C. Khan Goh, and Z. Ning Chen, "Impedance characterization of RFID tag antennas and application in tag co-design," *IEEE Trans. Microw. Theory Techn.*, vol. 57, no. 5, pp. 1268–1274, May 2009.
[38] H. H. Tran, S. X. Ta, and I. Park, "A compact circularly polarized crossed-dipole antenna for an RFID tag," *IEEE Antennas Wireless Propag. Lett.*, vol. 14, pp. 674–677, 2015.
[39] S. Bhaskar and A. K. Singh, "Linearly tapered meander line cross dipole circularly polarized antenna for UHF RFID tag applications," *Int. J. RF Microw. Comput.-Aided Eng.*, vol. 29, no. 5, May 2019, Art. no. e21563.
[40] M. Švanda and M. Polívka, "Horizontal five-arm folded dipole over metal screening plane for UHF RFID of dielectric objects," *Microw. Opt. Technol. Lett.*, vol. 52, no. 10, pp. 2291–2294, Jul. 2010.
[41] M. Polivka and M. Svanda, "Stepped impedance coupled-patches tag antenna for platform-tolerant UHF RFID applications," *IEEE Trans. Antennas Propag.*, vol. 63, no. 9, pp. 3791–3797, Sep. 2015.

TURKE ALTHOBAITI received the B.Sc. degree in computer science from Taif University, Saudi Arabia, in 2009, the M.Sc. degree in computer science from Ball State University, USA, in 2014, and the PhD degree in computer science from the University of the West of Scotland, U.K., in 2019. He is currently an Assistant Professor with Northern Border University, Saudi Arabia. His research interests include affective computing and machine learning.

ABUBAKAR SHARIF received the M.Sc. degree in electrical engineering from the University of Engineering and Technology, Lahore, Pakistan, and the Ph.D. degree in electronics engineering from the University of Electronic Science and Technology of China (UESTC). From 2011 to 2016, he worked as a Lecturer with Government College University Faisalabad (GCUF), Pakistan. He is also working as a Research Fellow with UESTC. He is the author of several peer-reviewed international journal and conference papers. His research interests include wearable and flexible sensors, compact antenna design, antenna interaction with the human body, antenna and system design for RFID, passive wireless sensing, and the Internet of Things (IoT).

JUN OUYANG received the Ph.D. degree in electromagnetic and microwave technology and the Post-Doctorate degree in information and signal processing from the University of Electronic Science and Technology of China (UESTC), in 2008 and 2011, respectively. He is currently working as an Associate Professor with the School of Electronic Science and Engineering, UESTC. He is also an Associate Director of the Smart Cities Research Center, UESTC. He is also a Research Fellow and the Chief Scientist of the Internet of Things Technology of Chengdu Research Institute. He is the author of more than 80 articles and 20 patents. Recently, he is leading several national-level research projects, provisional, and ministerial research projects. His research interests include antenna theory and design, microwave systems, RFID tag, wireless sensing, and the Internet of Things.

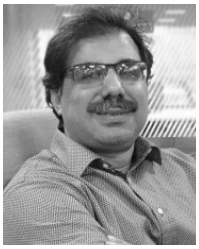

NAEEM RAMZAN (Senior Member, IEEE) received the M.Sc. degree in telecommunications from the University of Brest, France, in 2004, and the Ph.D. degree in electronics engineering from the Queen Mary University of London, London, U.K., in 2008.

He is currently a Full Professor of artificial intelligence and the Director of the Affective and Human Computing for Smart Environment (AHCSE) Research Center, University of the West of Scotland (UWS), U.K. He is also a Full Professor with the School of Computing, Engineering, and Physical Sciences, UWS. He coedited a book titled *Social Media Retrieval* (Springer, 2013). He has authored or coauthored over 110 research publications, including journals, book chapters, and standardisation contributions. He has authored or coauthored over 200 research publications, including journals, book chapters, and standardisation contributions. He authored a book and coedited some books as well. He has been a Lead Researcher in various nationally or EU sponsored multimillion-funded international research projects (total funding as PI secured over £20m). He has participated in more than 20 projects funded by European and U.K. research councils. His research interests include cross-disciplinary and industry focused and include: AI/machine learning, affective computing and multimedia processing, analysis and communication, video quality evaluation, brain-inspired multimodal cognitive technology, big data analytics, affective computing, the Internet of Things (IoT)/smart environments, natural multimodal human–computer interaction, and eHealth/connected health.

Dr. Ramzan is a Voting Member of the British Standard Institution (BSI). He is a Senior Fellow of the Higher Education Academy (HEA). He received the Best Paper Award 2017 of the IEEE TRANSACTIONS ON CIRCUIT AND SYSTEMS FOR VIDEO TECHNOLOGY and number of his conference papers were selected for the Best Student Paper Award. He has been awarded the Scottish Knowledge Exchange Champion Award 2020 and numerous other awards like Staff Appreciation and Recognition Scheme (STARS) Award for Leadership, in 2019, the STARS Award 2015 and 2017 for the Outstanding Research and Knowledge Exchange from UWS, and the Contribution Reward Scheme 2011 and 2009 for outstanding research and teaching activities from the Queen Mary University of London. He is the Co-Chair of the MPEG HEVC Verification (AHG5) Group. In addition, he holds key roles with the Video Quality Expert Group (VQEG) such as the Co-Chair of the Ultra High Definition (UltraHD) Group, the Visually Lossless Quality Analysis (VLQA) Group, and the Psycho-Physiological Quality Assessment (PsyPhyQA). He is a Co-Editor-in-Chief of the VQEG eLetter and served as a Guest Editor for a number of journals. He is the Founding Associate Editor of *Quality and User Experience* (Springer Journal) and an Associate Editor for the number of journals. He has chaired/co-chaired/organised more than 25 workshops, special sessions, and tracks in international conferences. He has developed a highly innovative portfolio of post graduate studies, including the M.Sc. advanced computing, the M.Sc. big data, the M.Sc. IoT, and the M.Sc. eHealth/digital health. He served as a guest editor for a number of special issues in technical journals. He has organised and co-chaired three ACM multimedia workshops and served as the Session Chair/Co-Chair for a number of conferences. He is the Co-Chair of the Ultra HD Group of VQEG.

QAMMER H. ABBASI (Senior Member, IEEE) received the B.Sc. and M.Sc. degrees (Hons.) in electronics and telecommunication engineering from the University of Engineering and Technology (UET), Lahore, Pakistan, and the Ph.D. degree in electronic and electrical engineering from the Queen Mary University of London (QMUL), U.K., in January 2012.

From 2012 to June 2012, he was Postdoctoral Research Assistant with the Antenna and Electromagnetics Group, QMUL. From 2012 to 2013, he was an International Young Scientist under the National Science Foundation China (NSFC) and an Assistant Professor with UET, KSK. From August 2013 to April 2017, he was with the Center for Remote Healthcare Technology and Wireless Research Group, Department of Electrical and Computer Engineering, Texas A&M University at Qatar (TAMUQ), initially as an Assistant Research Scientist and later was promoted to an Associate Research Scientist and a Visiting Lecturer. He is currently a Lecturer (an Assistant Professor) with the School of Engineering, University of Glasgow. In addition, he is also a Visiting Lecturer (an Assistant Professor) with QMUL. He has grant portfolio of around £4.5M, contributed to a patent and more than 320 leading international technical journal and peer-reviewed conference papers, in addition to ten books, he received several recognitions for his research. His research interests include nano communication, the Internet of Things, 5G and its applications to connected health, RF design and radio propagation, RFID, applications of the millimeter and terahertz communication in healthcare and agri-tech, wearable and flexible sensors, compact antenna design, antenna interaction with human body, implants, body centric wireless communication issues, wireless body sensor networks, noninvasive health care solutions, and physical layer security for wearable/implant communication.

Dr. Abbasi is a member of the IEEE 1906.1.1 Standard Committee on Nano Communication and IET and a Committee Member of the IET Antenna and Propagation and Healthcare Network. He has been a member of the technical program committees of several IEEE flagship conferences. He was the Chair of the IEEE Young Professional Affinity Group. He is an Associate Editor of IEEE Access journal, the IEEE Journal of Electromagnetics, RF and Microwaves in Medicine and Biology, the IEEE Sensors, and the IEEE Open Journal of Antenna and Propagation. He acted as a Guest Editor for numerous special issues in top notch journals, including *Nano Communication Network* (Elsevier). He has been a technical reviewer for several IEEE and top-notch journals. He contributed in organising several IEEE conferences, workshop, and special sessions in addition to European school of antenna course.